Results in Engineering 28 (2025) 107213

Contents lists available at ScienceDirect

Results in Engineering

journal homepage: www.sciencedirect.com/journal/results-in-engineering

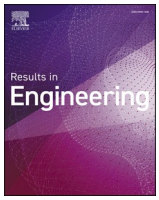

Research paper

Using machine learning to compute tire-penetration related properties for enhanced rolling resistance prediction

W.A.A.S. Premarathna [a], Kumar Anupam [a,*], M. Moenielal [b], Thijs Wensveen [c], Cor Kasbergen [a], Sandra M.J.G. Erkens [a]

[a] Section of Pavement Engineering, Faculty of Civil Engineering and Geosciences, Delft University of Technology, Stevinweg 1, 2628 CN, Delft, Netherlands
[b] Section of Buildings, Materials and Structures, TNO, Molengraaffsingel 8, 2628 JD Delft, Netherlands
[c] Section of Intelligent Imaging, TNO, Oude Waalsdorperweg, Den Haag, Netherlands

ARTICLE INFO

Keywords:
Greenhouse gas emissions (GHG)
Rolling resistance
Surface texture
Climate change
Tire- pavement interaction
Asphalt pavements
Enveloping technique
Tire penetration
Laser crack measurement system (LCMS)

ABSTRACT

A major contributor to GHG emissions is the transportation sector, particularly pavement transport. The limited understanding of tire-pavement interactions leads to inaccurate predictions of these emissions, particularly from rolling resistance (RR). Traditional methods for predicting RR are constrained by their limited applicability and inability to account for the complex dynamics of tire-pavement interactions, resulting in poor prediction accuracy. These limitations make it challenging for policymakers to make proper decisions, as existing methods are manual and labour-intensive. This study aims to develop an automated system to capture tire-pavement interaction data using the Laser Crack Measurement System (LCMS). To the best of the authors' knowledge, no robust technique currently exists for automatically calculating tire penetration-related information from LCMS data to predict RR. Therefore, this research explores machine learning (ML)-based models to reduce uncertainties in existing approaches and enhance RR predictions using automated LCMS data. It examines the relationships between RR, tire penetration volume, and the characteristics of the Dutch pavement network, comparing the results with those of commonly used RR prediction models. The study introduces an automatic tire penetration calculation approach using LCMS data to assess the impact of tire penetration volume and depth on RR in relation to surface properties. The findings reveal that traditional empirical models show poor correlations between RR and texture indicators, whereas ML-based models significantly improve the accuracy of RR predictions. These results could inform the development of strategies to reduce GHG emissions from pavement transport, supporting global efforts to combat climate change and achieve the goals of the Paris Agreement.

1. Introduction

Human-generated greenhouse gas (GHG) emissions from the consumption of fossil fuels are one of the major contributors to global warming [1]. Recent reports [2,3] indicate that GHG emissions has not been sufficiently controlled in accordance with the Paris agreement of 2015. The GHG emissions still need to be reduced by 28 % to 42 % to achieve the aim of limiting the temperature increase to 1.5 °C to 2 °C [3,4]. The key contributors of GHG emission are transportation sector, industrial sector, energy sector, etc. [5]. Contribution from the transportation sector is crucial because >95 % of transportation still relies on fossil fuels [6]. Vehicles moving on roads are responsible for 70 % of direct transport emissions [7,8]. The engine efficiency of vehicles, aerodynamics, rolling resistance, inertia effects, mechanical frictions, traffic and characteristics of the pavement surface are key factors that play a considerable role in direct transport emissions [8–10].

Recent studies [11,12] have highlighted the importance of rolling resistance which significantly affects to the emissions. However, the issues related to the rolling resistance have not been solved because the lack of deeper understanding of tire-pavement interaction behaviour. One of lack of success in relation to the rolling resistance is the inaccurate consideration of tire-penetration volume [13]. Additionally, insufficient correlations between surface morphology and rolling resistance hinder scientific efforts to optimize tire and pavement engineering designs [13,14]. The gaps in understanding result in poor predictions of rolling resistance, which will ultimately lead to inaccuracy in the overall GHG emissions.

Surface texture parameters of pavements are used to quantify and

* Corresponding author.
E-mail address: K.Anupam@tudelft.nl (K. Anupam).

https://doi.org/10.1016/j.rineng.2025.107213
Received 25 June 2025; Received in revised form 1 September 2025; Accepted 9 September 2025
Available online 10 September 2025

describe the characteristics of pavement surface morphology. Empirical models were mostly developed using well-known surface texture parameters and roughness parameters to describe their statistical relationship with rolling resistance, such as Mean Profile Depth (*statistical MPD*), Root Mean Square (*statistical RMS*), Estimated Texture Depth (*statistical ETD*), Skewness (*statistical*), and the International Roughness Index (*statistical IRI*) [10,15]. The models have been introduced by using single and/or multivariable combinations of texture parameters to predict rolling resistance [16–19]. Predictions of the models rely on the correlations between texture parameters of surface at the macro-texture level and rolling resistance [10,17,20–22]. The empirical models often ignore the contribution of tire such as effect of tire related factors to rolling resistance and focus solely on pavement characteristics in their predictions.

In modern days many road organizations use automatic methods to compute texture properties. One of the most commonly adopted automated technology is Laser Crack Measurement System – LCMS [23]. Although LCMS has been utilized by a few researchers [23,24] to calculate texture-related properties such as MPD, RMS, etc., its direct relationship to rolling resistance has not been studied. Apart from the above parameters, scientific efforts have not been made to identify other parameters that could help improve the prediction of rolling resistance. Therefore, to the best of the authors' knowledge, LCMS data has not yet been utilized to improve the prediction of rolling resistance.

Past studies [21,25–28] reveal that commonly used rolling resistance prediction models only with texture parameters are unable to accurately predict rolling resistance. Though, some statistical models provide reasonable correlation results, such models are only applicable for predicting rolling resistance under specific pavement types or limited testing and operating conditions [18,29,30]. Also, transferability of the models is difficult due to their limited ability to effectively interpret the partial envelopment of the tire tread interaction with different pavement textures [28,31]. Therefore, combination of both physical tire-pavement representations with conventional techniques is one approach to improve the prediction of rolling resistance [13,31,32]. However, the complexity of physical tire-pavement interaction with the limited literature, make it difficult to find a proper solution for better prediction of rolling resistance.

In recent years, machine learning (ML) techniques have been extensively used to successfully predict outcomes from physical tire-pavement interaction, such as noise and skid resistance [33,34]. The ability of the ML techniques to manage massive datasets can help overcome some of the limitations of commonly used rolling resistance prediction models. However, to the best of the authors' knowledge, there is no/limited ML-based framework to predict rolling resistance by incorporating pavement surface properties and tire related parameters. In response to the background of the study and identified limitations, the following subsection outlines the aim, objective and scope of the research.

1.1. Research goal and scope

The primary goal of this study is to develop an ML-based framework to evaluate improvements in rolling resistance prediction by considering the relationships between rolling resistance, and texture properties. In addition to this, a secondary goal is to explore the relationship between tire-pavement interaction and rolling resistance using LCMS data. Together, these objectives aim to advance the accuracy of rolling resistance prediction while also providing new insights into the role of surface characteristics in tire-pavement interaction. The proposed ML-based framework is developed using multiple linear regression (ML-MLR) and random forest regressor (RF) models [35–38], as these models are widely used in the literature for similar applications [36,38–40]. The RF model is selected due to its strong ability to capture non-linear relationships, robustness to overfitting, and effectiveness with limited or noisy datasets. In contrast to complex models such as neural networks, RF provides a good balance between accuracy and interpretability without requiring large amounts of training data or extensive hyperparameter tuning.

As discussed in the previous sections, the tire penetration volume as identified by previous researchers [41,42] is an important parameter for improving the prediction of rolling resistance. The tire penetration volume is typically defined as the level of depth or volume intrusion of the tire tread into pavement cavities in relation to surface morphology [41,42]. Integrating tire penetration volume with existing surface texture properties is expected to provide deeper insights into the relationship between tire properties and surface macro-texture parameters. However, measuring an accurate value of the parameter and understanding its relationship with rolling resistance are practically impossible. Texture measurement via LCMS allows for accurate prediction of tire penetration volume. However, to the best of the authors' knowledge, predicting tire penetration volume and improving the prediction of rolling resistance using LCMS still remains an unsolved problem. In order to address above problem and achieve the aim, the scope of the research is defined as follows:

i. To understand the validity of commonly used rolling resistance prediction models in terms of the prediction accuracy of rolling resistance using surface texture information derived from historical data. The relevant data are gathered in Dutch pavement network. Sections with PA16 (ZOAB / ZOAB+) are chosen, because PA16 is the most common asphalt top layer used on highways in the Netherlands. It is noted that the purpose of selecting only a single type of top layer is to get a more consistent dataset, with fewer variables that might influence rolling resistance. The main focus on this step is to provide a foundation for evaluating the reliability of existing popular models.
ii. The study examines the association between rolling resistance and surface texture information derived from LCMS data. Clustering and correlation analyses is performed to explore the relationships between rolling resistance, pavement surface age, pavement surface type, and surface texture indicators, offering insights into key influencing factors with the use of LCMS.
iii. By leveraging an enveloping technique, it seeks to understand the way of surface texture information captured by LCMS data correlates with rolling resistance, enhancing the understanding of above intricate relationships as described by (i) and (ii). The study delves deeper into the specific contribution of tire penetration volume to rolling resistance prediction.
iv. To improve the accuracy of rolling resistance predictions, ML-MLR and RF models will be developed. The study provides ML models that incorporate correlations between tire-related factors and pavement texture information, offering robust predictive tools based on insights from the preceding analyses.

1.2. The novelty of the research

The innovative aspects of the research are highlighted below:

i. *Application of machine learning for tire-pavement interaction:* the research introduces a machine learning-based framework for predicting rolling resistance by moving beyond conventional statistical and empirical methods. As an early application of ML models, including ML-MLR and RF, it explores the complex interactions between tire characteristics, pavement texture and rolling resistance.
ii. *Use of comprehensive LCMS data:* the study leverages data from the LCMS, which provides in-depth texture information that supports a thorough analysis of pavement surface characteristics, enabling robust ML model development. To the best of the authors' knowledge, none of the previous studies have emphasized the use of LCMS data in rolling resistance prediction.

iii. *Holistic approach combining pavement and tire characteristics:* the study provides a more holistic approach to improve the understanding of rolling resistance by combining pavement texture indicators with tire penetration volume data.
iv. *Implications for policy and engineering modifications:* the insights gained through this study can inform policy-making and engineering practices by providing a clearer understanding of the way that tire and pavement characteristics contribute to rolling resistance, potentially guiding future adjustments in pavement and tire design.

1.3. Structure of the paper

The paper is organized to highlight the relationship between rolling resistance, texture indicators and tire penetration volume by using LCMS data and machine learning techniques. The study first discusses current approaches for predicting rolling resistance. Then a research framework is established which outlines the study's aim, scope and methodology. The findings are analysed and interpreted in the results and discussion section. The results highlight the relationship between tire penetration volume and rolling resistance. In the subsequent sections, the paper presents improved prediction accuracy of rolling resistance using machine learning models. Finally, the paper presents a summary of the key insights and future research directions.

2. Current approaches for predicting rolling resistance

This section explores key aspects related to rolling resistance prediction that are currently popular in pavement engineering community. First, commonly used prediction models for rolling resistance are reviewed while highlighting their drawbacks. Secondly, the significant factors related to tire-pavement interaction are discussed. After that, the importance of using ML models for predicting rolling resistance are examined.

2.1. Commonly used prediction models of rolling resistance

The prediction of RR is an essential component of current studies, as not everything can be tested, and various aspects require calibration and validation. Therefore, RR prediction models play an important role. Commonly used predictive models can be found in previous studies [10,43]. As given in Table 2.1, most of the relationships between rolling resistance coefficient (*RRC*) and texture parameters are simple linear statistical models. However, as evident in Table 2.1, most models fail to account for the complex non-linear relationships between tire and pavement related factors. ML models can be incorporated to overcome limitations of commonly used rolling resistance prediction models. The ML models have proved their capabilities to handle the complex non-linear problems compared to linear regression-based models [44]. Which will be discussed in the following sub-Section 2.2.

2.2. Incorporating machine learning models

Machine learning models possess the ability to identify complex non-linear relationships more effectively than linear regression-based models presented in Table 2.1 [59–61]. Within the pavement engineering, researchers have developed ML models for texture-related parameters to improve pavement maintenance procedures, innovate new asphalt mixtures, and predict skid resistance [62–67]. ML models have not been developed to predict rolling resistance considering both tire and pavement properties. Hence, only limited number of studies are discussed in this sub-section in-relation to the development of ML models using the texture-related parameters.

Zhan et al. [68] proposed an integrated fast Fourier transform and ML models-based framework to predict pavement skid resistance from 3D texture measurements by comparing the prediction accuracy of different ML-based models. A recent study utilized RF-based machine learning model and pavement micro and macro-texture characteristics to improve the friction prediction of pavement surfaces [69]. Apart from the pavement's macro and micro characteristics, International Roughness Index (IRI) is a commonly used index that quantifies pavement roughness, and it directly correlates with the comfort, rolling resistance and road safety [10,70]. A random forest regression model was developed to predict the IRI of flexible pavements using distress measurements, traffic, climatic, maintenance, and structural data [71]. The study's findings demonstrated that the RF model significantly outperformed the linear regression model in both the training and test sets under limited dataset. A study compared the performance of three machine learning algorithms such as artificial neural network, random forest, and support vector machine with traditional techniques based on the predicted IRI. The results indicated that the random forest model provided the highest accuracy, achieving an overall performance value of 0.995 [72]. Further details on the development of machine learning models using texture and other pavement related parameters can be found in other sources [73,74].

2.3. Importance of tire penetration volume

The tire penetration volume is defined in relation to the volume of rubber penetrated to the surface texture and corresponding pavement

Table 2.1
Commonly use rolling resistance prediction models.

Rolling resistance prediction model	Model number	Key observations
$RRC = C_1 \times MPD + C_2$ (2.1)	Model 1	A direct linear relationship between *RRC* and *MPD* was assumed. The model considered only the impact of *MPD* on *RRC*, ignoring other potential surface-related factors such as *RMS* or *Skewness* [10,17].
$RRC = C_1 \times RMS + C_2$ (2.2)	Model 2	Instead of *MPD* variable in model 1, the model 2 used *RMS* as the independent variable to predict *RRC*. It hypothesized that *RRC* is directly proportional to the *RMS* [10,17].
$RRC = C_1 \times MPD + C_2 \times RMS + C_3 \times Skewness + C_4$ (2.3)	Model 3	Compared to the above model 1 and model 2, multiple predictors such as *MPD*, *RMS*, and *Skewness* were added to the model 3. By including Skewness, the model aimed to account for the asymmetry in the surface profile distribution, making it more robust for complex surface textures [10,17].
$RRC = C_1 \times MPD + C_2 \times \left(\frac{MPD}{RMS}\right) + C_3$ (2.4)	Model 4	Introduced a term $\left(\frac{MPD}{RMS}\right)$, which might help to capture specific interactions or dependencies between *MPD* and *RMS* [10,17].
$RRC = C_1 \times MPD + C_2 \times RMS + C_3 \times Skewness + C_4 \times \left(\frac{MPD}{RMS}\right) + C_5$ (2.5)	Model 5	The model 5 combined all predictors and terms to form a fully detailed representation. The model was developed to capture complex relationships and interactions among the surface texture parameters, providing maximum flexibility [10,17].

where, C_1, C_2, C_3, C_4 and C_5 are coefficients generally determined.

texture profiles [31]. Studies have been conducted in the past that try to relate the contribution of the penetration volume to tire-pavement friction [45–50]. However, it is noted that none of them have studied rolling resistance. The tire penetration volume can be used to understand the way of tires interact with varied pavement surfaces in different operating conditions. Researches [45,49,52] have shown that when sliding the rubber of the tire at low velocities on the surface texture, the rubber undergoes deformation in a way that perfectly conforms to the short-wavelength surface texture profile of the substrate. Under low velocity conditions, the tire rubber contacts only 5 % of the pavement surface [45,51]. When considering longer length scales, the contact includes the most prominent surface irregularities of the pavement. Within this contact region, the local pressure is significant enough to compress the rubber material into numerous smaller-sized cavities [45,46]. Hence, the tire penetration volume would change depending on the specific length scale of the selected pavement profile. Such variation in tire penetration volume generates fluctuating forces on the rubber surface, resulting in energy dissipation through the internal friction of the rubber [45,54]. The magnitude of hysteresis forces increases which contribute to the rolling resistance due to the changes as mentioned above [45,54].

The changes in the tire penetration volume as mentioned in the previous paragraph can be governed by different factors such as, the sharpness of the texture summits, the type of pavement, and the hardness of the rubber [31]. The variations occur due to changes in summits because the contact interactions between the sharp summits (or positive texture) and the smooth summits (or negative texture) result in distinct responses from the tire rubber during the penetration process [31]. Under identical load and surface conditions, a tire tread composed of hard rubber exhibits lower penetration into surface cavities on the pavement compared to a tread with a smoother rubber composition [31]. The type of pavement significantly changes the true contact area between the tire and the pavement and thereby the tire penetration level [31,53]. Researchers [54–56] have identified additional factors such as tire's width, tire pressure, and the rubber's modulus which also contribute to the tire penetration level. Apart from factors highlighted previously, recent studies [50,57,58] have identified the directional characteristics of the pavement texture, traffic direction, and polishing effect could contribute to the change of tire penetration volume.

2.4. Summary of key highlights of existing approaches

On the basis of the details mentioned in the above sections, following key highlights are identified.

i. The Laser Crack Measurement System is widely used to compute texture properties such as MPD, RMS, etc., but it has not yet been utilized to predict rolling resistance. Additionally, the parameters measured using LCMS and their direct connection to rolling resistance remain unexplored.
ii. Most commonly used relationships between rolling resistance and texture parameters are based on linear regression models. It has been identified that the models overlook tire-related factors and fail to capture the complex interactions between the tire and pavement.
iii. ML models are able to capture complex, non-linear relationships better than traditional statistical linear regression-based models.
iv. Machine learning has been successfully applied in pavement engineering for texture analysis, skid resistance prediction, and pavement maintenance improvements. According to ML-based predictions in most studies in pavement engineering, random forest models outperform other ML algorithms, even with limited datasets.
v. Despite the advancements in ML models, there are still no or very few ML models for directly predicting rolling resistance by considering both tire and pavement properties.
vi. In order to improve the prediction accuracy of rolling resistance, the tire penetration volume can be incorporated into the models as a key parameter representing tire-pavement interaction.
vii. The overall understanding of rolling resistance can be enhanced by incorporating both pavement texture indicators and tire penetration volume data into the analysis.
viii. The tire penetration volume can be utilized as a more effective indicator for addressing the interaction between the tire and the texture of the pavement surface.
ix. The tire penetration volume is a tangible and physics-based parameter, as opposed to numerical methods such as enveloping algorithms.
x. Being a composite variable, the tire penetration volume accounts for multicollinearity attributes. It introduces less bias and consequently reduces uncertainties in rolling resistance predictions.
xi. It is also feasible to capture the influence of changing environmental conditions on rolling resistance, including variations in temperature, as well as wet and dry surface conditions.

3. Research methodology

As illustrated in Fig. 3.1, the study was conducted in five main phases. In Phase I, data collection in the field and data processing were carried out. In Phases II to IV, the relationships between preliminary prediction models, tire penetration volume and ML models with rolling resistance were obtained. In Phase V, the significance of the outcomes from Phases II to IV was compared, and the results were presented. A description of tasks performed in each phase is described in following sub-sections.

3.1. Data mining

In Phase I, data such as LCMS data, rolling resistance data and historical information were collected from Dutch road network and processed the data to conduct analyses mentioned in the steps from Phase II to Phase V. A total number of 18,782 data records were collected for the model development and analysis. Using the gathered data, data preprocessing was performed to conduct data cleaning and data validation. Steps such as standardization, data filtering, etc. were followed to ensure the quality of the gathered data while also enabling correct transformation for further analysis.

3.1.1. Types of pavement sections

The pavement surface texture data were collected using LCMS measurements [75] and field measurements on pavement surfaces (see sub-Section 3.1.2 and sub-Section 3.1.3). The rolling resistance data for pavement surface sections were gathered using TU-Gdansk's rolling resistance measurement trailer [76] for passenger cars. The surface texture data were also gathered simultaneously with the rolling resistance measurements.

3.1.2. Types of pavement sections

Research [43] concluded that there is a significant impact of surface texture on the rolling resistance experienced by vehicles on Dutch highways. Researchers [43] showed that within 95 % confidence level pavement surfaces with finer gradation (0/5, 0/6) results in 9–11 $\pm$ 2 % lower rolling resistance as compared to the average rolling resistance values of PA16 surfaces. The study used PA16 and dense asphalt pavement sections as given in Table 3.1, where both rolling resistance and texture measurements were measured [77]. The measurements were taken along a 500 m length on each of the pavement sections, with total 12 measurement runs.

It is noted that the selected pavement surfaces vary in age and maintenance condition. The rolling resistance data of PA16 and dense asphalt pavement sections were collected utilizing rolling resistance

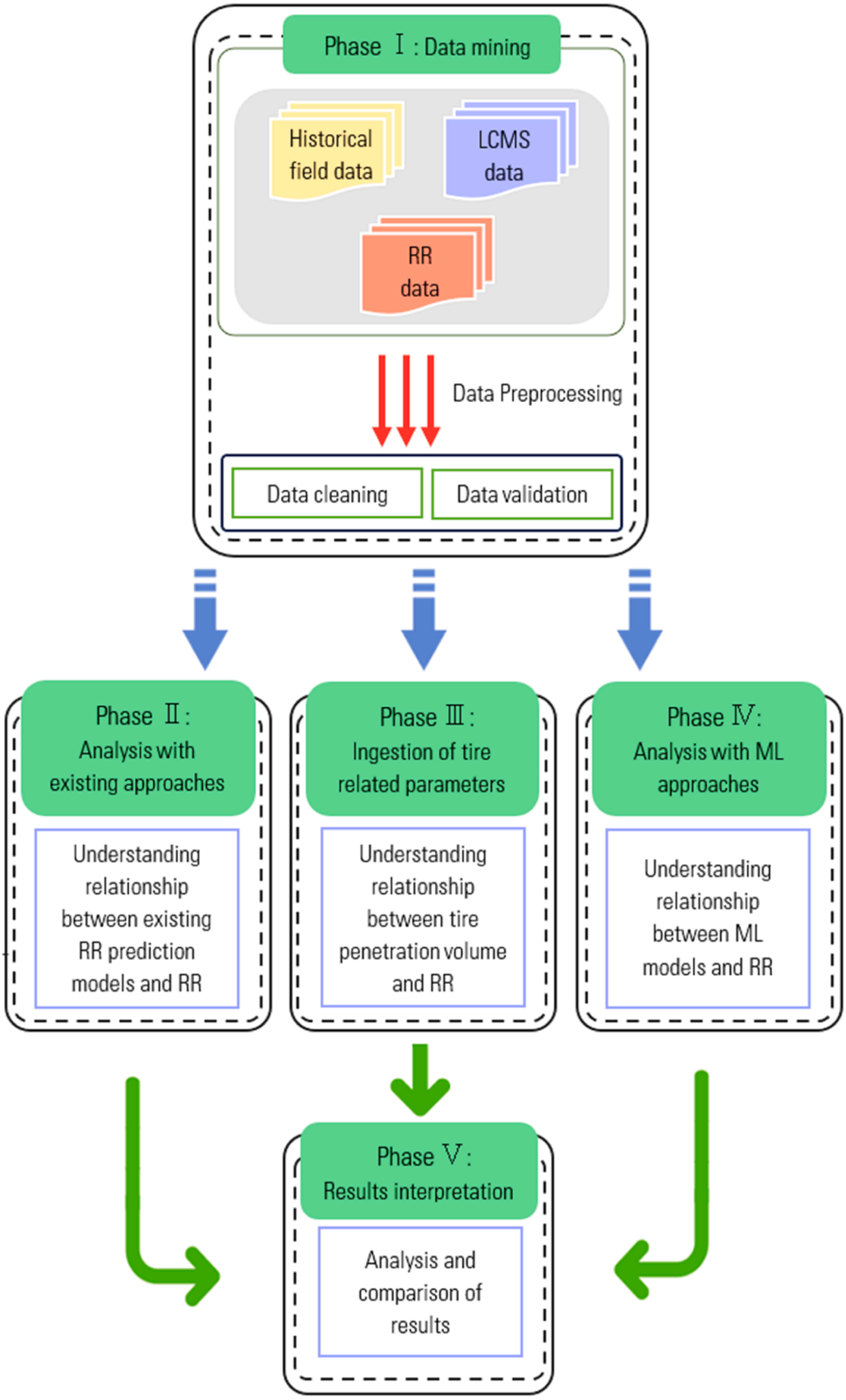

Fig. 3.1. Process framework innovation.

Table 3.1
Description of PA16 and dense asphalt pavement sections.

Acronym	Expanded form (Dutch)	Expanded form (English)
DAB	Dicht Asfaltbeton	Dense Asphalt Concrete
DGD	Dunne Geluidsreducerende Deklaag	Double Graded Dense Asphalt Concrete
EAB	Emulsie Asfaltbeton	Emulsion Asphalt Concrete for Dense Surface Layers
OAB	Open Asfaltbeton	Open Asphalt Concrete
ZOAB	Zeer Open Asfaltbeton	Porous Asphalt
ZOAB+	Zeer Open Asfaltbeton +	Porous Asphalt +
ZOABTW	Zeer Open Asfaltbeton Tweelaags	Double Layered Porous Asphalt
ZOEAB	Zeer Open Emulsie Asfaltbeton	Emulsion Asphalt Concrete for Porous Asphalt

measurement trailer [28,76]. The texture measurements were measured using laser crack measurement system [78]. As shown in Table 3.1, both Dutch and English acronyms are provided to facilitate understanding for both national and international pavement engineering communities.

3.1.3. Field surveys from laser crack measurement system

LCMS uses a single-pass 3D laser line triangulation sensor. It is noted that modern LCMS data offers a comprehensive 1 mm resolution, while historical data of the Dutch highway system is available at 1 by 5 mm resolution. More information of LCMS can be found elsewhere [78]. As demonstrated in Fig. 3.2, texture profile lines taken from the raw LCMS data are used to determine *MPD* values. It is noted that cross profiles with 1 mm resolution were utilized, as length profiles were only accessible in 5 mm resolution. A cross profile of 100 mm serves as the baseline in *MPD* calculation. With a *MPD* value calculated every 250 mm and subsequently averaged to obtain a value every 5 m

3.1.3.1. LCMS and rolling resistance data alignment. The test dataset was obtained from the LCMS measurements to minimize the number of variables and noise. The aim was to maximize the chance of finding a reliable correlation between the rolling resistance field data and properties derived from the raw LCMS data. The criteria such as type of the asphalt top layer, GPS coordinates and age of the pavement were considered when selecting the dataset for the analyses. To enhance the reliability of the test dataset, sections with aligned data sources for both rolling resistance field data and raw LCMS data were selected. The measurement locations were matched by using the GPS data. Furthermore, similar age of the pavements was selected to collect the data.

3.1.4. Field measurements

Field measurements of historical field data were acquired utilizing the measurement system at a speed of 80 km/h. The data from measurement system were to compute relevant texture indicators including *MPD*, *RMS*, *ETD*, and *Skewness* [79]. The components of the system are presented in Table 3.2.

3.1.5. Rolling resistance field measurements and prediction

In order to measure the rolling resistance, TU-Gdansk's rolling resistance measurement trailer [28,76] was used at a speed of 80 km/h as recommended by previous research [26]. The SRTT (Standard Reference Test Tire) [82] was mounted to the trailer with the pressure of 2.1 bars. In each test, a so-called warm-up process was conducted on the tire, so that temperature stabilization, material flexibility, and pressure equalization could be achieved, ensuring consistent and reliable test results. Throughout the tests, tire pressure and temperature were continuously monitored by a sensor attached to the tire, which wirelessly transmitted data to the data acquisition system. The sensor with accuracy of ± 0.01 bar provided a real-time monitoring and adjustment of tire pressure as necessary. As tire pressure was actively monitored during testing, no manual adjustments were made during the measurements. In addition to above measurements, surface temperature and surrounding air temperature were also accounted to the database. More details about field measurement procedures and specifications can be found elsewhere [43].

Table 3.2
Key components of the surface texture measuring system.

Serial no	Components	Type	Accuracy	Measurement range	Sampling range
1	Speedometer	Corrsys L-350 Aqua (Corrovit) [80]	1.5 mm distance, 0.2 % speed	0.3 - 250 km/h	–
2	Laser triangulation sensor	LMI laser 2207–64/180-G [81]	0.07 mm	64 mm	48 kHz

3.2. Rolling resistance analysis with existing approaches

In phase II, rolling resistance was predicted by employing commonly used rolling resistance prediction models and processed data in Phase I. The analyses were carried out using simple linear regression-based models, multiple linear regression-based models, and also, varied sampling approaches. The results of the rolling resistance predictions were compared with the outcomes in Phase III and Phase IV.

3.3. Ingestion of tire related parameter and understand the relation with rolling resistance

In Phase III, the relationship between surface texture properties, tire penetration volume and rolling resistance was analysed using LCMS data. Using artificially generated surface texture, enveloping techniques, and the methodology described by [31], the tire penetration volume was calculated. The volume of deformed rubber was calculated from the raw LCMS depth data by selecting a 50 × 50 mm patch around the wheel track. Computing the volume of pixels at a given depth from the highest point in the patch the volume of deformed rubber was obtained.

3.4. Analysis with machine learning-based approaches

In phase IV, data science techniques and ML models were utilized to predict rolling resistance and identify correlations between surface texture properties. As discussed in sub-Section 2.2, rolling resistance was predicted using RF and ML-MLR models as ML-based toolkit.

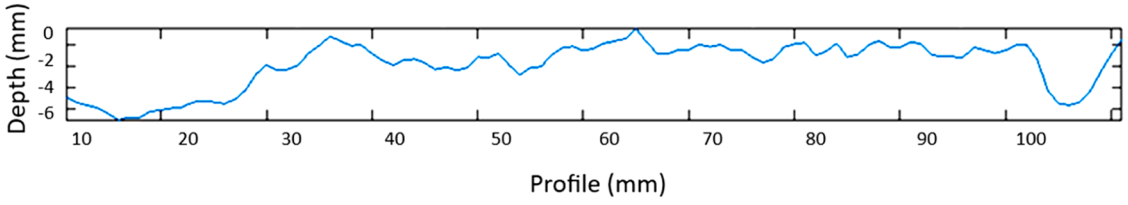

Fig. 3.2. Texture profile from raw LCMS data (1 mm resolution).

3.5. Analysis and results interpretation

In Phase V, an evaluation was performed based on the outcomes from Phase II to Phase IV which is discussed in following sections.

4. Results and discussions

The results, obtained in different phases of the research as shown in Fig. 3.1, are discussed in this section. At first, the improvements of the rolling resistance predictions by including the varied sampling regression-based models are compared against traditional approaches. Next section evaluates the relationships between pavement characteristics and rolling resistance using LCMS data. The LCMS data were further used to identify the correlations between tire penetration volume and rolling resistance. Finally, the prediction accuracy of rolling resistance and its correlation with pavement characteristics were studied using machine learning models.

4.1. Investigation of commonly used models excluding varied data sampling technique

The prediction capabilities of the existing statistical regression-based rolling resistance models (see Table 2.1) were evaluated on the basis of field data. The analysis was carried out using both simple linear regression-based models and multiple linear regression-based models without considering varied data sampling technique.

4.1.1. Investigation of simple linear regression-based prediction models

As shown in Figs. 4.1(a) - (c), the highest coefficient of determination (R^2) value between *RRC* and *MPD* was 0.22. Moreover, the relationship between *RMS* against *RRC*, and *Skewness* against *RRC* were also showed a poor R^2 values of 0.09 and 0.03, respectively. Hence, it can be concluded that the none of the parameters, such as *MPD*, *RMS* and *Skewness*, has a significant linear relationship with *RRC*.

4.1.2. Investigation of multiple linear regression-based prediction models

Data presented in Fig. 4.2 were further evaluated using multiple linear regression-based prediction models to identify possible improvements in predictions. As given in Table 4.1a, models 3, 4 and 5 showed a moderate relationship with *RRC* because Multiple R was 0.5 and R^2 values below or equal to 0.273 indicating 72.7 % of a significant portion of other important factors were not included in the models. Moreover, R^2 values for the three models were below 0.3 suggesting that the proposed relationships were not effectively correlated with *RRC*. Further detail of statistical parameters used in this study can be found elsewhere [83]. In order to further investigate the significancy of the parameters in the models, ANOVA-based statistical analysis was conducted. As given in Table 4.1b, models 3 and 4 demonstrated strong statistical significance and reliability of the estimations because the both models indicated small standard errors and lower p-values. The parameter with Variable 2 in model 3 showed a negative effect, all the Variables in model 4 displayed consistently positive relationship, while model 5 showed weaker statistical significance ($p = 0.468$). The larger standard errors of model 5 indicated its less precise estimation capabilities. Overall, models 3 and 4 appeared to be a better choice with respect to model 5.

4.2. Investigation of commonly used models including varied data sampling technique

As discussed in Sub-Section 4.1, the correlations between *RRC* and various texture parameters showed a poor correlation in terms of R^2. In order to overcome the effect of the outliers and random fluctuations in the dataset, as proposed by researchers [84–86], the data points were averaged over 10 m of pavement sections. This was done under the hypothesis that the sampling technique improves the accuracy of the prediction by reducing measurement noise, minimizing local variability, and enhancing the signal-to-noise ratio.

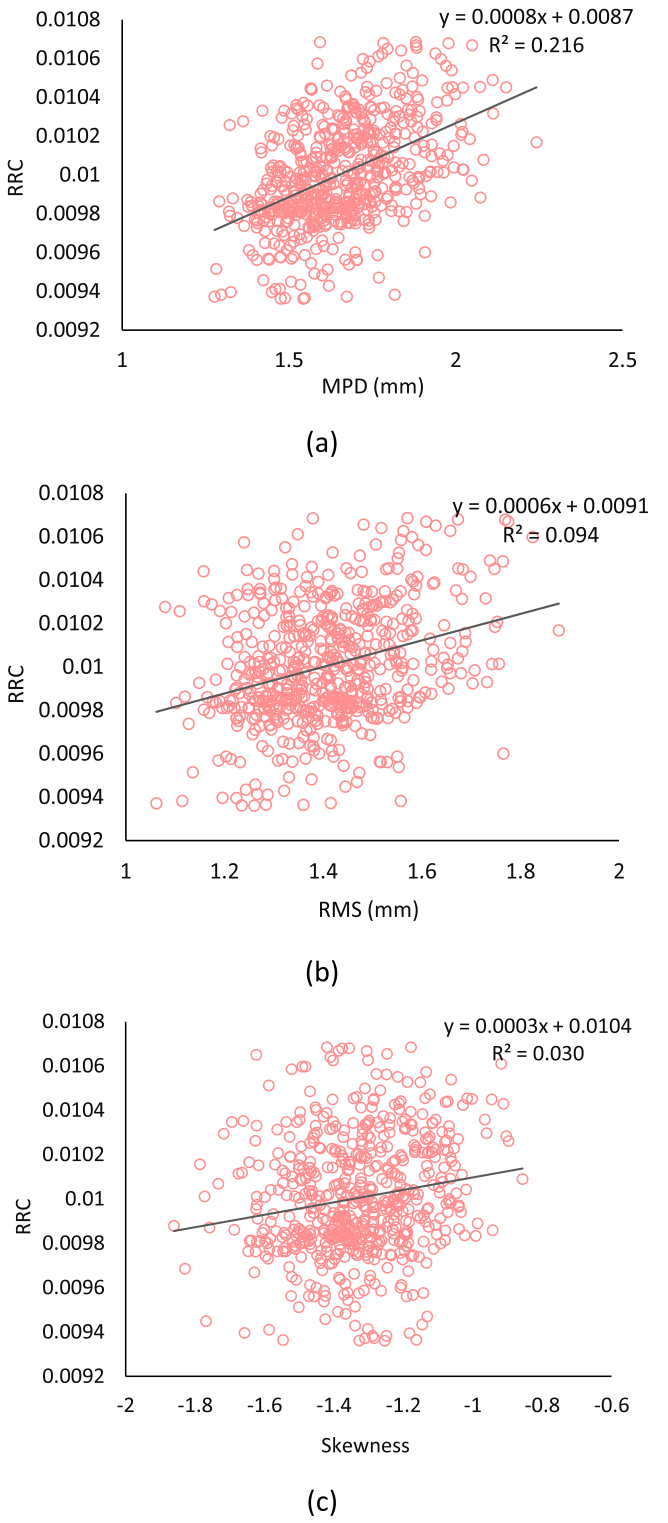

Fig. 4.1. Relationships between rolling resistance and texture parameters: (a) relation between rolling resistance and mean profile depth, (b) relation between rolling resistance and root mean square, and (c) relation between rolling resistance and skewness.

4.2.1. Investigation of simple linear regression-based models including varied data sampling technique

Figs. 4.2(a) - (c) show the relationships between *RRC* and *MPD*, *RMS*,

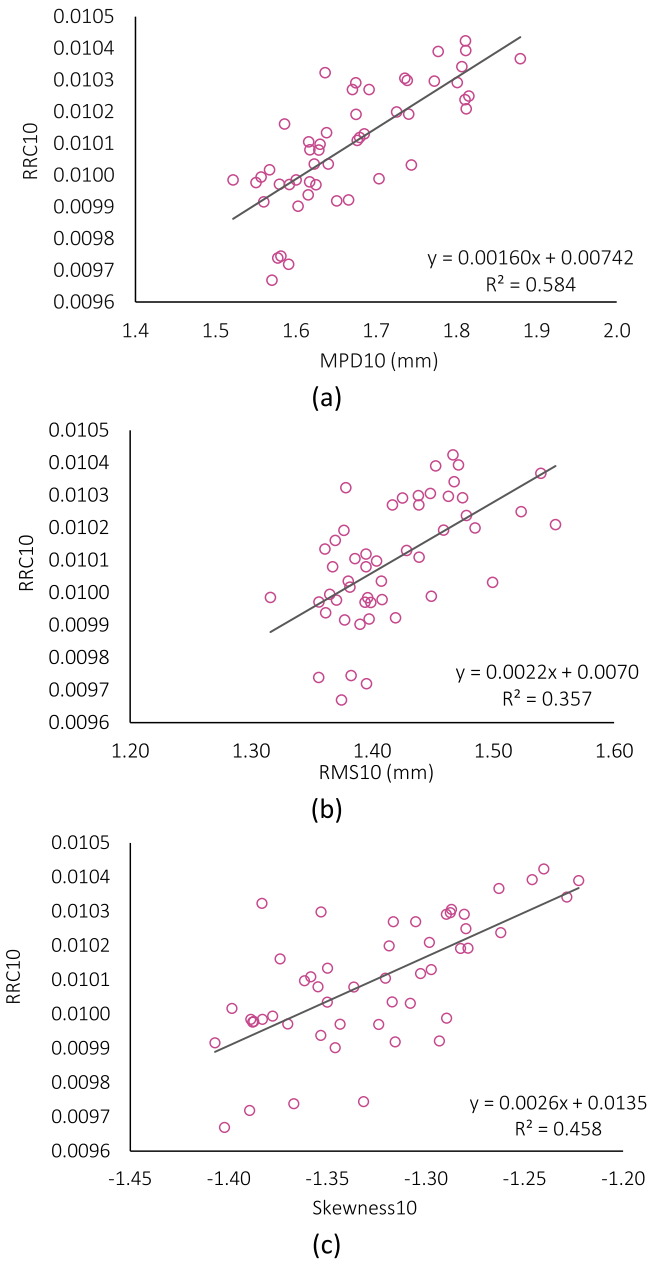

Fig. 4.2. Relationships between rolling resistance and texture parameters with varied sampling technique: (a) relation between rolling resistance and mean profile depth, (b) relation between rolling resistance and root mean square, and (c) relation between rolling resistance and skewness.

Skewness that were obtained using the averaged sampling technique. In the corresponding figure, y-axis represents *RRC*10 and x-axis represents different texture parameters such as *MPD*10, *RMS*10 and *Skewness*10 to indicate the use of averaged sampling data. *RRC*10, *MPD*10, *RMS*10, and *Skewness*10 represent the averaged rolling resistance coefficient data, averaged mean profile depth, averaged root mean square, and averaged skewness data over a sampling distance of 10 m, respectively. The R^2 was found to be 0.58 for *MPD* against *RRC* and 0.36 and 0.46 for *RMS* against *RRC* and *Skewness* against *RRC*, which is a slight improvement over the previous approach.

4.2.2. *Investigation of multiple regression-based models including varied data sampling technique*

Table 4.2 presents a comparison of the prediction accuracies of *RRC* including and excluding the varied sampling technique. The R^2 of model 3 increased from 0.25 to 0.65, while the R^2 increased by 0.41 and 0.38 for models 4 and 5, respectively. The Mean Squared Error (MSE) and Mean Absolute Error (MAE) decreased across all three models. Overall, it can be concluded that there is a moderate relationship between *RRC* and texture parameters which were obtained through the varied sampling technique.

As shown in Table 4.3, Cohen's f^2 was used to calculate the effect size of the results computed in three models, both including and excluding the data from the varied sampling technique. The comparison was made by measuring the incremental contribution of one model over another using Cohen's f^2 values. The calculated effect sizes indicated that the incremental contribution of model 4 relative to model 3 was negligible ($f^2 = -0.011$), while the addition of predictors in model 5 resulted in a small effect compared to both model 4 ($f^2 = 0.039$) and model 3 ($f^2 = 0.028$).

Similarly, the effect sizes of the models including data from the varied sampling technique were slightly larger than those of the models excluding such data. Model 5, including data from the varied sampling technique, showed a small-to-moderate incremental effect compared to both model 4 ($f^2 = 0.059$) and model 3 ($f^2 = 0.041$). Moreover, model 4, including the varied sampling data, contributed minimally compared to model 3 ($f^2 = -0.017$). Overall, the comparison indicates that the models including data from the varied sampling technique have higher explanatory power and slightly stronger incremental effects than the models excluding the data. The largest gains in effect size were observed when moving from model 4 to model 5 in both datasets, suggesting that the predictors added in model 5 meaningfully enhance model performance.

4.3. *Investigation of improved prediction of rolling resistance using ML models*

As discussed in sub-Sections 4.1 and 4.2, the commonly used models did not provide a good relationship with *RRC*. Therefore, the next approach was to utilized ML-based methods to predict the *RRC*, which could find hidden relationships between hidden parameters. First, Pearson's correlation analysis was conducted to understand the

Table 4.1a
Summary output of multiple regression.

Model	Item	df	SS (1×10^{-5})	MS (1×10^{-6})	F	Significance F (1×10^{-39})	Multiple R[1] (1×10^{-3})	R^2	Adj. R^2	Std. Error (1×10^{-4})
3	Regression	3	1.1	3.600	66.55	0.045	503	0.25	0.26	2.0
	Residual	590	3.2	0.054	–	–	–	–	–	–
	Total	593	4.3	–	–	–	–	–	–	–
4	Regression	2	1.0	5.200	95.62	0.001	494	0.24	0.24	2.3
	Residual	591	3.3	0.054	–	–	–	–	–	–
	Total	593	4.3	–	–	–	–	–	–	–
5	Regression	4	1.2	2.900	55.24	1.500	522	0.27	0.27	2.3
	Residual	589	3.1	0.052	–	–	–	–	–	–
	Total	593	4.3	–	–	–	–	–	–	–

[1] Multiple R evaluates the model's ability to predict the dependent variable [83].

Table 4.1b
Summary output of ANOVA test.

Model	Parameter	Coefficients	Std. Error (1×10^{-4})	t-Stat.	p-value	Lower 95 %	Upper 95 %
3	Intercept[1]	0.009	1.6	52.662	0.000	0.008	0.009
	X Variable 1	0.001	1.4	10.104	3.3×10^{-22}	0.001	0.002
	X Variable 2	−0.001	1.6	−5.360	1.2×10^{-7}	−0.001	−0.001
	X Variable 3	0.000	0.8	−3.144	1.7×10^{-3}	4.0×10^{-4}	4.0×10^{-4}
4	Intercept	0.008	1.8	44.646	0.000	0.008	0.008
	X Variable 1	0.001	0.6	10.665	2.1×10^{-24}	0.001	0.001
	X Variable 2	0.001	1.6	4.684	3.5e-6	4.3×10^{-4}	0.001
5	Intercept	0.001	20.0	0.726	0.468	−0.002	0.005
	X Variable 1	−0.003	10.0	−2.620	0.009	−0.005	-7.0×10^{-4}
	X Variable 2	0.004	10.0	3.290	0.001	0.002	0.007
	X Variable 3	−0.003	0.8	−3.437	0.001	-4.1×10^{-4}	-1.1×10^{-4}
	X Variable 4	0.006	20.0	4.022	6.5×10^{-5}	0.003	0.009

[1] The Intercept and X Variables 1, 2, 3, and 4 are all significant predictors of the dependent variable [83].

Table 4.2
Comparison of the multiple regression models including and excluding varied sampling technique.

Model	Parameter	Value of parameters	
		Results of regression statistic – excluding varied sampling technique	Results of regression statistic – including varied sampling technique
3	Multiple R	0.503	0.805
	R^2	0.253	0.649
	Adjusted R^2	0.249	0.626
	Standard Error	0.230	0.110
	Observations	594	59
	MSE	0.410	0.210
	MAE	1.164	0.612
4	Multiple R	0.494	0.804
	R^2	0.244	0.646
	Adjusted R^2	0.242	0.631
	Standard Error	0.230	0.110
	Observations	594	59
	MSE	0.471	0.199
	MAE	1.168	0.598
5	Multiple R	0.522	0.806
	R^2	0.273	0.650
	Adjusted R^2	0.268	0.618
	Standard Error	0.230	0.110
	Observations	594	59
	MSE	0.371	0.208
	MAE	1.158	0.598

Table 4.3
Cohen's f^2 effect sizes for incremental contributions of models including and excluding varied data sampling technique.

Comparison of models	Effect size (f^2) excluding varied data sampling technique	Effect size (f^2) including varied data sampling technique
Model 4 vs Model 3	- 0.011	- 0.017
Model 5 vs Model 4	0.039	0.059
Model 5 vs Model 3	0.028	0.041

relations between the multiple features and execute the dimensionality reduction in the dataset. As shown in Fig. 4.3, the legend represents different colours with varying intensity levels, indicating the strength of correlations between features. The colour intensity is varying in the cells from low (0) to high (+1 or −1). Low colour intensity cells indicate no correlation while high density of colours signify a strong positive correlation, or a strong negative correlation between features in the dataset.

As shown in Fig. 4.3, the texture indicators *ETD*, *RMS* and tire inflation level features exhibited high correlation with the *MPD* indicator, with Pearson correlation coefficients of $r_{ETD} = 1$ and $r_{RMS} = 0.94$, respectively. Features of air temperature and road temperature correlated with tire temperature. A strong positive correlation (0.94) between *MPD* and *RMS* indicates that an increase in *MPD* results in a corresponding increase in *RMS*, and vice versa. A correlation coefficient of 1 between *MPD* and *ETD* suggest a significant linear relationship, which imply both metrics essentially measure the similar aspect of pavement surface texture. Therefore, *MPD* and *ETD* provide an equivalent information regarding texture depth.

The correlation values on the corresponding figures indicate that *MPD*, *RMS* and *ETD* are dependent variables. Consequently, *MPD* is sufficient for further analysis in this study as it adequately represents *RMS* and *ETD* without significant loss of information. The model dimensions were reduced by selecting *MPD*, *Skewnees*, *Tire temperature*, *Tire inflation pressure* as the representative key features for the subsequent analyses.

According to feature rankings by relative importance (Fig. 4.4), temperature-related features have the greatest influence on rolling resistance, with *Tire temperature* (24 %), *Road temperature* (17.4 %), and *Air temperature* (14.9 %) ranking highest, followed by *Tire inflation pressure* (9.4 %). Pavement texture features play a smaller role in comparison, where *MPD* (11.9 %) and *ETD* (11.3 %) are more important than *Skewnees* (5.9 %) and *RMS* (5.2 %). Overall, temperature-related variables dominate over pavement texture features in terms of importance. As explained in the research scope and methodology sections, the ML-MLR and RF models were used to develop the ML-based rolling resistance prediction model using key features.

4.3.1. Performance of multi linear regressor models

The dimensionally reduced dataset was divided into three sets such as training, validation, and testing according to recommendations of past researchers. 60 % of the data was allocated for training the two ML models of ML-MLR and RF, 20 % for validation, and 20 % for testing. Hyperparameter tuning for the ML models was performed using Randomized Search CV due to its ability to deliver faster results within the training set. However, a known limitation [87,88] of Randomized Search CV is that it evaluates only a random subset of hyperparameter combinations, so the optimal configuration may not always be identified. Consequently, the validation set was employed to systematically monitor performance consistency and detect potential overfitting, while the test set was reserved exclusively for final model evaluation. As shown in Fig. 4.5(a), the low adjusted R^2 of 0.56 indicates that the multi linear regression model was not capable of capturing the complexity of the relationships between the features and the *RRC*. In other words, although multiple linear regression-based was able to handle multiple features, it was not able to capture non-linear behaviour between the features and the target variable (*RRC*).

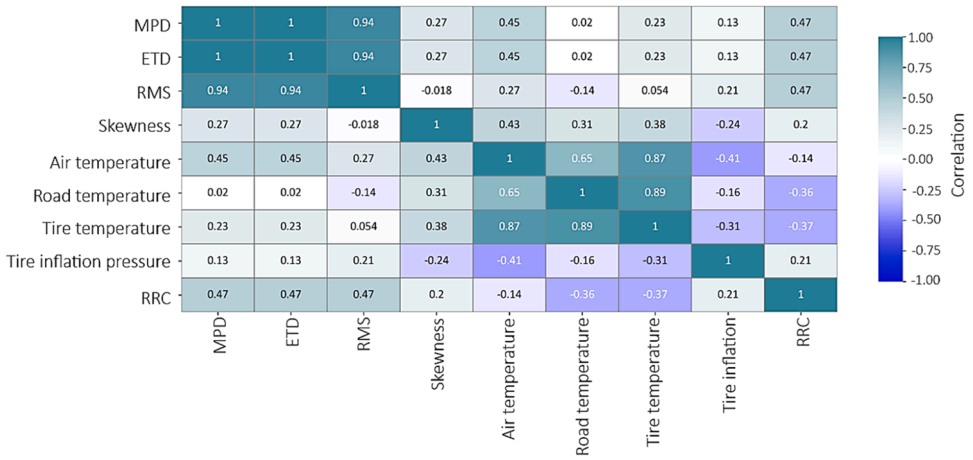

Fig. 4.3. Correlation heat map with highly correlated features.

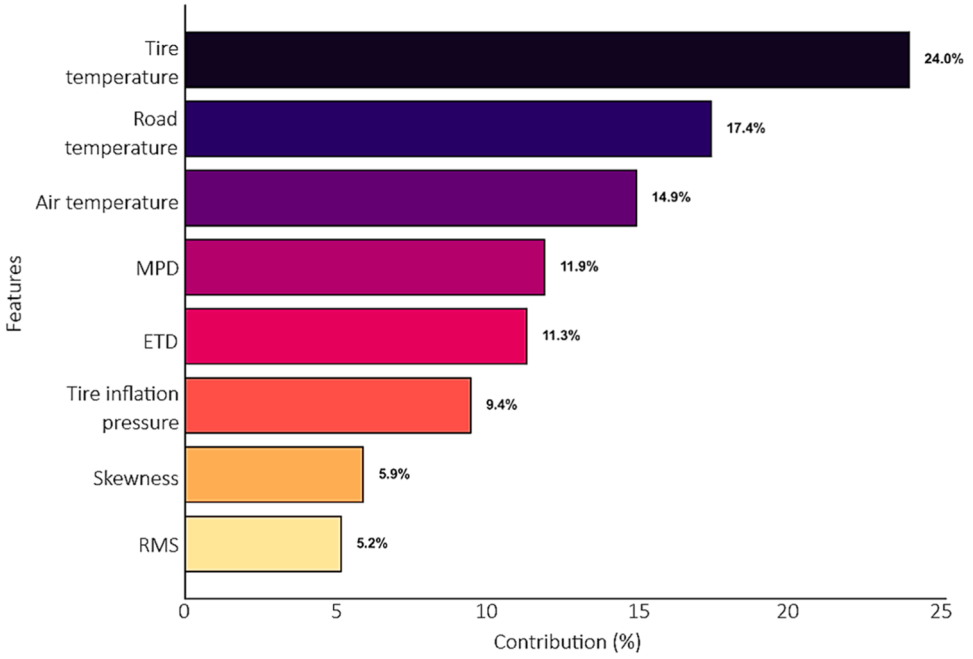

Fig. 4.4. Feature rankings by relative importance, expressed as a percentage of total importance. The most influential features are shown at the top, with relative contributions indicated by bar length and percentage labels.

4.3.2. Performance of random forest regressor models

As discussed earlier, the prediction accuracy of ML-MLR model showed a lower accuracy. The next approach was to utilized advance ML model such as RF model. The comparison of actual and predicted *RRC* values by using RF model is shown in Fig. 4.5(b) and Fig. 4.5(c). Fig. 4.5 presents the predicted RRC values based on the test set. The high adjusted R^2 of 0.84, along with the relatively low MSE of 0.051 and MAE of 0.164, indicates that the RF was capable of capturing the complexity of the relationships between the selected features and the rolling resistance coefficient. In other words, RF model was able to capture non-linear behaviour between the features and the target variable (*RRC*). Fig. 4.5(c) shows the comparison of *RRC* data which were measured in field and predicted by RF model. In order to provide a better visibility of the data points, only data points within 500 m are presented in the corresponding figure.

To evaluate the model's robustness, a 5-fold cross-validation was performed by using randomized search CV. The obtained CV scores and estimated best estimator's parameters of the RF are presented in Table 4.4. According to Table 4.3, the average CV score coupled with a low standard deviation demonstrates that the model performs consistently across different subsets of the validation data with minimal variance.

The error (*RRC* field data - *RRC* predicted data) was high for linear regressor ML model and it could be a reason of the limited prediction capability of that specific model. In contrast, the RF model provided better prediction with low error. The results from commonly used models and results from ML models showed significant differences, especially results of RF. Hence, it can be concluded that the ML techniques can be helped to overcome the difficulties that have been encountered in the commonly used rolling resistance prediction models.

Prediction uncertainty for the RF model was quantified using a bootstrap resampling approach. 100 bootstrap samples of the training dataset were generated (with replacement). For each resample, a RF model was retrained, and the distribution of predictions was obtained. The 2.5th and 97.5th percentiles of the prediction distribution were used to construct 95 % prediction intervals for the test set. The bootstrap

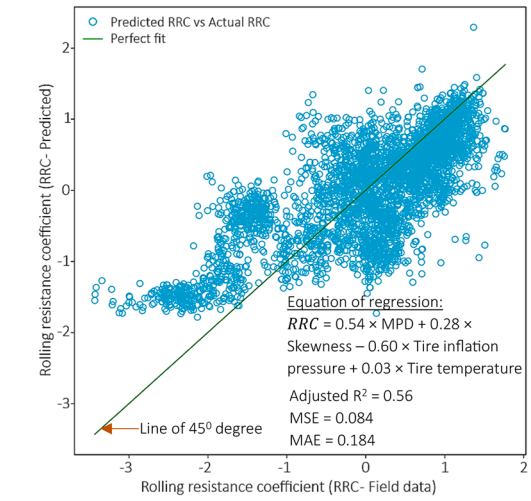

(a)

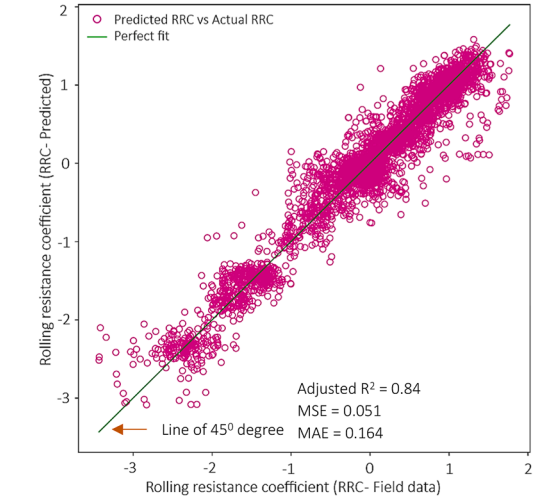

(b)

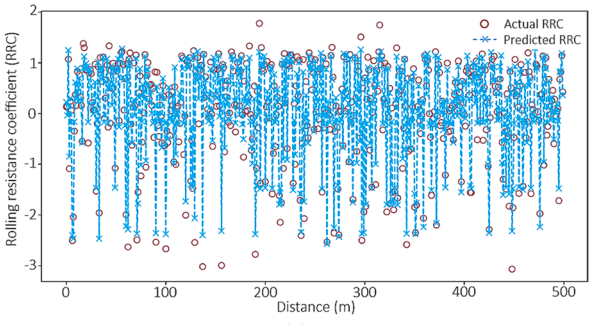

(c)

Fig. 4.5. Relationship between actual rolling resistance coefficient test data and predicted rolling resistance coefficient values: (a) comparison of multiple linear regression model-based rolling resistance coefficient values, (b) comparison of random forest model-based rolling resistance coefficient values, and (c) comparison of rolling resistance coefficient values with respect to distance. Note that the values on the dependent and independent axes are presented after standardization.

analysis produced relatively narrow prediction intervals, with an average 95 % CI width of 0.109. The results indicate limited variability in the model's predictions and supports the robustness and reliability of the RF outputs.

Table 4.4
Parameters estimated from Cross-Validation (CV).

Estimator/Parameter	Parameter value
Cross-Validation scores	0.0577, 0.0549, 0.0548, 0.0577, 0.0557
Mean Cross-Validation	0.0562
Standard deviation of Cross-Validation	0.0013
Best estimator	RandomForestRegressor(max_depth=10, max_features='sqrt', min_samples_leaf=5, min_samples_split=5, n_estimators=900, random_state=42)

Overall, when compared to both conventional models and ML-based models, it is evident that ML-based models outperformed traditional approaches, as previously discussed. This improvement of the performance can be attributed to the ability of ML-based models to identify complex, hidden patterns and relationships within the given data. In the comparison between the ML-MLR model and other statistical models, the ML-MLR model showed a marginally higher accuracy, with an average improvement of 0.31 over statistical models that did not incorporate varied sampling techniques. However, when varied sampling techniques were included, the performance of the ML-MLR model was comparable to that of the statistical models. Furthermore, the RF model better predictive performance, surpassing the ML-MLR model by 0.28 in terms of improved prediction accuracy.

4.4. Investigation of pattern recognition in rolling resistance using LCMS data

As shown in the previous sections, ML models, particularly the RF model, significantly outperformed the other models. However, the relationships remain hidden or within a black box. To further improve prediction accuracy, incorporating more physical information is necessary. As discussed in Sections 2 and 3, including parameters such as pavement type, tire penetration volume, and pavement age could enhance prediction accuracy. These features are crucial in engineering applications and could have significant importance for the tire industry and pavement sector. Pattern recognition in this context can help identify key features. The influence of texture properties, tire penetration volume, and pavement age on RRC was investigated using LCMS data. The tire penetration depth and *MPD* were calculated by applying the enveloping technique to the texture profiles in the LCMS dataset [31]. As shown in Fig. 4.6. During the calculation process the smaller "dips" in the profiles were excluded in the envelop because the dips could result in different and lower *MPD* values.

As shown in Fig. 4.7(a), different pavement surfaces resulted in different clustering patterns when *MPD* was computed against the *RRC*. The majority of the ZOAB surfaces showed a high *RRC* compared to rest of the surface types. This in line with the finding of the previous studies [10,17] as recommended due to higher air voids the *RRC* could be higher. As shown in Fig. 4.7(b), similar observations were made when the enveloped profile included. The *MPD* showed a slightly scale down values compared to the observations made using Fig. 4.7(a). A clear clustering pattern was not identified with respect to the *MPD* calculated on enveloped profile against *RRC* under different surface types. However, as presented in Fig. 4.7(c), *MPD* values from both LCMS-field data and enveloping technique showed a good agreement.

The relationships between *MPD*, *RRC*, and the age of the top layer were evaluated as shown in Fig. 4.8(a) – Fig. 4.8(c) It was observed that varying pavement ages led to distinct clustering patterns when *MPD* was plotted against *RRC*. It can be concluded from the patterns that newer pavement surfaces have lower rolling resistance compared to older surfaces. This could be due to the fact that older surfaces can degrade over time through rutting and ravelling, wearing and weathering resulting in uneven areas. Uneven surfaces can cause greater vibration and shock to the tires, increasing tire deformation and, consequently,

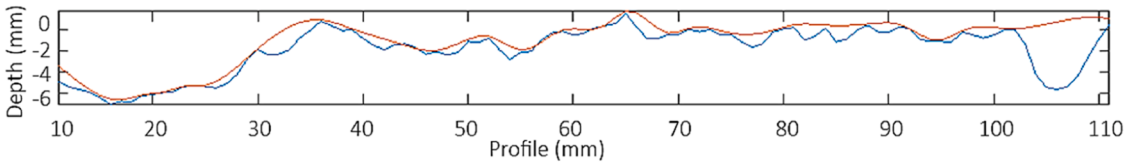

Fig. 4.6. Texture profile with envelope.

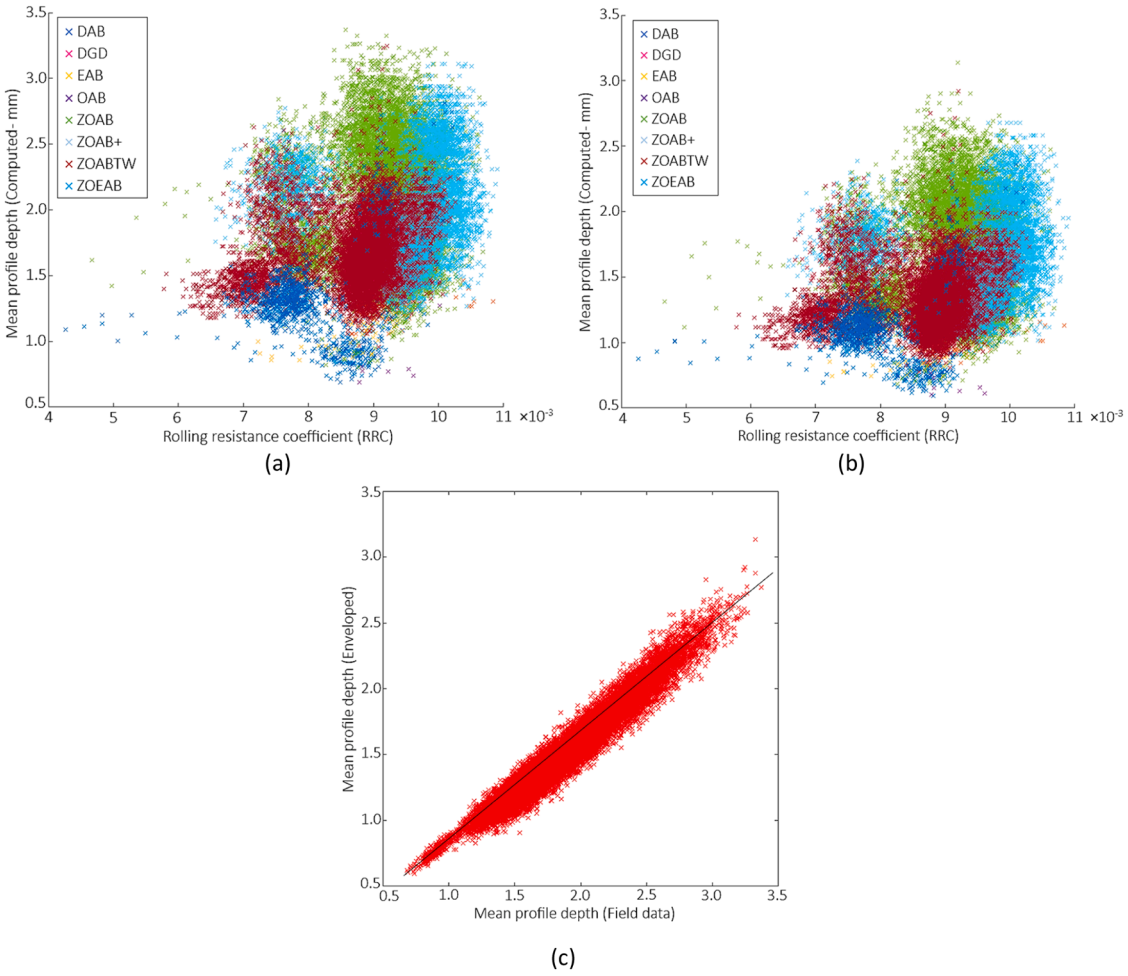

Fig. 4.7. Scatter plot of mean profile depth and rolling resistance coefficient by pavement surface type: (a) *MPD* calculated on raw LCMS-based profile, and (b) *MPD* calculated on enveloped profile, and (c) Mean profile depth calculated from raw and enveloped profiles.

leading to higher rolling resistance. In contrast, newer surfaces are smoother and aggregates are more evenly distributed, which can result in lower rolling resistance. Hence, it can be concluded that pavement age is an important parameter that can be incorporated into prediction models to improve the accuracy of rolling resistance predictions.

4.4.1. Framework for automatic calculation of tire penetration using LCMS data

As discussed in previous sub-sections, the results excluding the tire-pavement related parameters did not improve the predictions. Hence, as discussed in the methodology, the tire penetration volume and tire penetration depth were studied to evaluate the significance of these parameters on *RRC*. Due to variability in texture parameters, environmental conditions and tire properties, it is impossible to determine the exact value of tire penetration depth in practice. In this study, the corresponding values of penetration depth and volume of deformed rubber were calculated incorporating the enveloping technique. As shown in Fig. 4.9, a penetration depth of 2 mm results in a significantly lower penetration volume.

Furthermore, as the penetration depth decreases below 2 mm, the role of the tire penetration depth and deformed volume on tire-pavement interaction diminishes. Therefore, in order to reflect realistic values in the field, and considering that the average *MPD* of typical porous asphalt is ≈2 mm [89,90], a depth range between 2 mm and 6.5 mm was selected for this study. As shown in Fig. 4.9, as the tire penetration depth increases, the volume of deformed rubber also increases. This is in line with previous findings [54,91], as a greater penetration depth results in more rubber conforming to the texture profile.

The result proves the methodology for obtaining reliable information from LCMS data for penetration depth analysis. In order to better understand the influence of penetration depth, Fig. 4.10 was plotted, where the required volume of rubber was plotted against the penetration depth.

To facilitate better understanding, the *RRC* coefficients were divided into different sets from L_1 to L_4, starting from 0.008 and increasing in increments of 0.0005 up to 0.01. The selection of these ranges and the

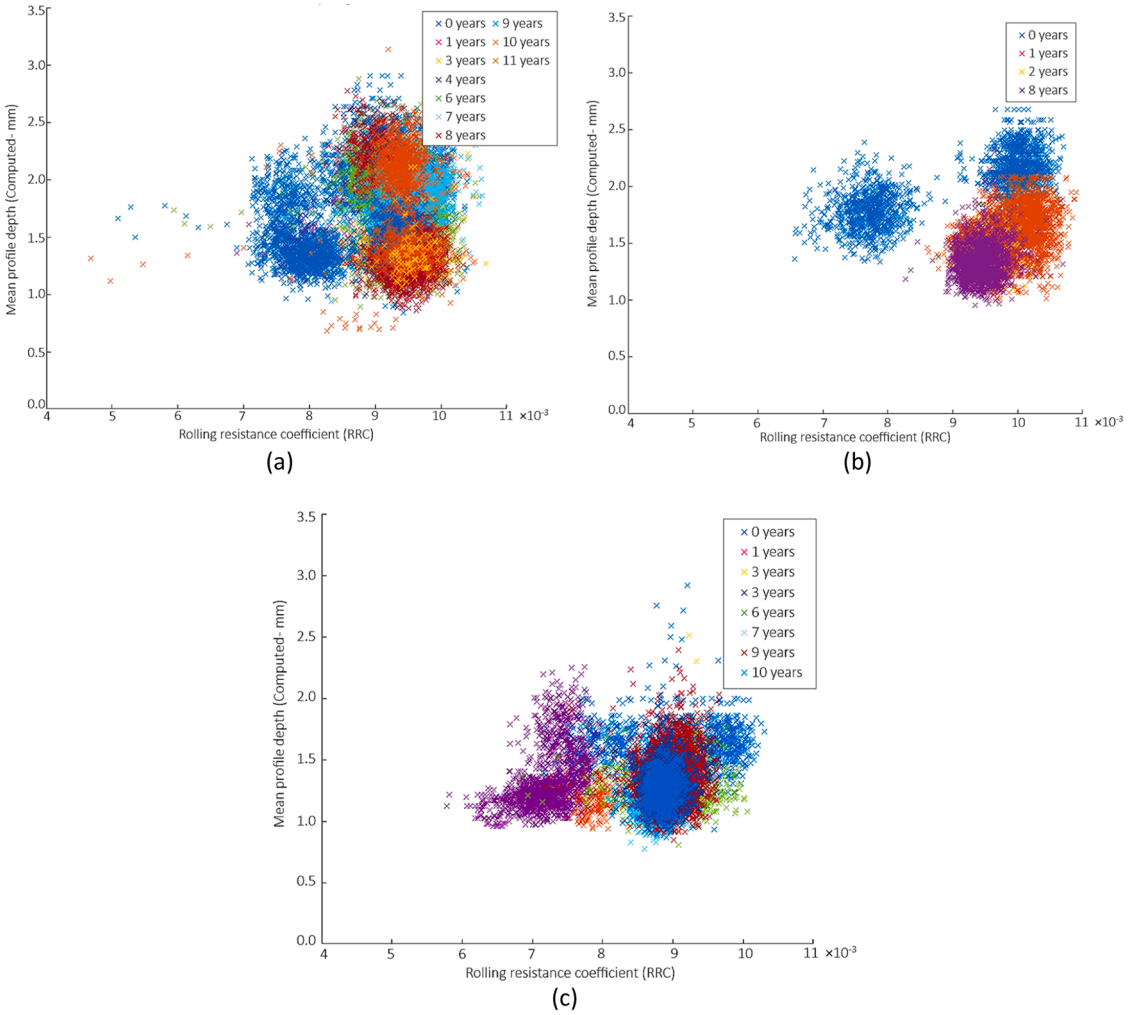

Fig. 4.8. Relationships between *MPD*, *RRC*, and the age of the top layer: (a) mean profile depth and rolling resistance coefficient for ZOAB with age, (b) mean profile depth and rolling resistance coefficient for ZOAB+ with age, and (c) mean profile depth and rolling resistance coefficient for ZOABTW with age.

specific increment size was based on the need to encompass all *RRC* values obtained from the dataset while ensuring sufficient resolution for data analysis. As an example, if the penetration depth is fixed at 5.4 mm, it can be seen that for L_4, a penetration value of 3 mm^3 is required. However, for the same penetration depth, L_2 shows rubber volume ranging from 1.2 mm^3 – 3.55 mm^3, which is not an expected trend. The trends are inconsistent across different penetration values, which is not in line with the hypothesis. The expected range for L_1, L_2, L_3, and L_4 is also reversed in relation to penetration depth and deformed volume. The averaged value for each set is expected to be in line with the order of $L_4 < L_3 < L_2 < L_1$. Therefore, the results disprove the hypothesis.

The discrepancy of the trends could be due to the limited dataset, where *RRC* only varied from 0.008 to 0.01. Additionally, penetration depth and volume were calculated using the enveloping technique based on LCMS data by applying an imaginary surface, as mentioned in previous sections.

5. Conclusions

This study evaluated the prediction accuracy of *RRC* using commonly used statistical models, machine learning (ML) techniques and LCMS data. The results revealed significant improvements when incorporating varied data sampling techniques and ML-based models, highlighting the limitations of commonly used regression-based methods in practice. This could be one of the reasons hindering the development of policies on rolling resistance, which is an important environmental concern. On the basis of the results and analysis presented in this paper, the following conclusions could be drawn:

i. *Investigation of commonly used regression-based models*: Simple linear regression- based models exhibited poor correlation with *RRC*, as indicated by low R^2 values. Multiple linear regression-based models showed moderate improvement, suggesting that a substantial portion of relevant factors affecting *RRC* were not captured. The ANOVA-based analysis further confirmed that models 3 and 4 exhibited stronger statistical significance compared to model 5.

ii. *Investigation of varied data sampling technique:* To enhance prediction accuracy, varied data sampling techniques were applied, resulting in a moderate increase in R^2 values and a decrease in MSE and MAE. Simple linear regression-based models with varied sampling showed improved correlations. Additionally, models based on multiple regression with varied sampling demonstrated improved performance. These results suggest that the improvement in prediction is not merely due to a reduction in data variance, but reflects better generalization and enhanced reliability of the models. Overall, these findings indicate that applying appropriate data sampling techniques can mitigate noise and improve the robustness and predictive accuracy of regression models. While the application of varied data sampling

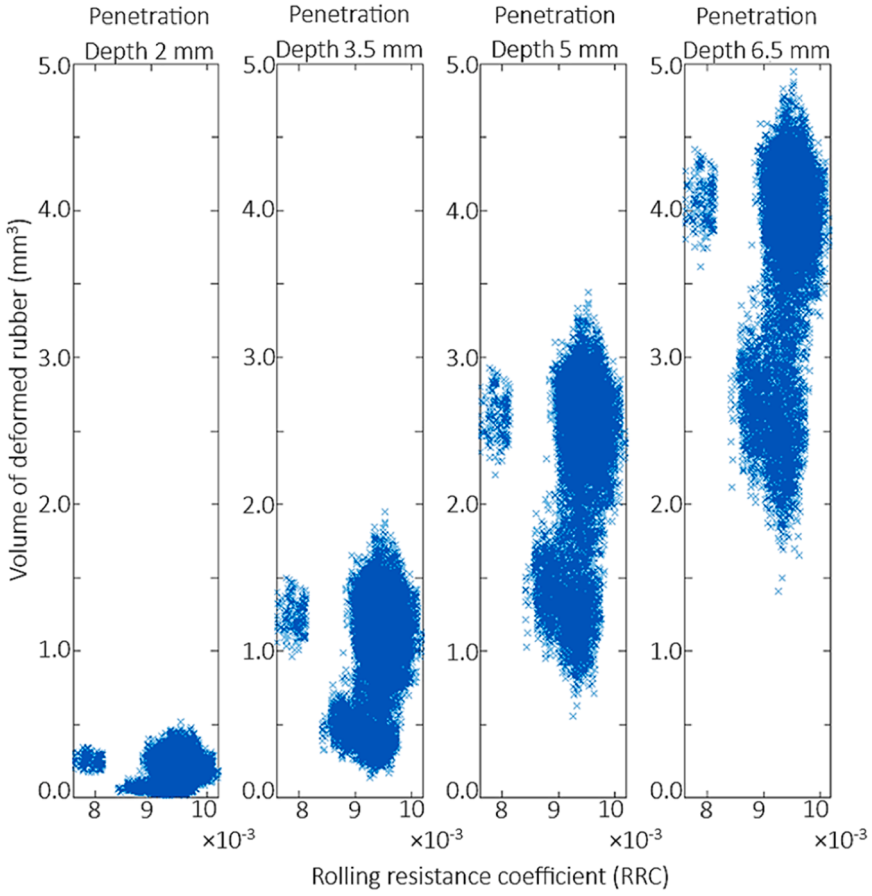

Fig. 4.9. Volume of deformed rubber for several penetration depths vs rolling resistance coefficient.

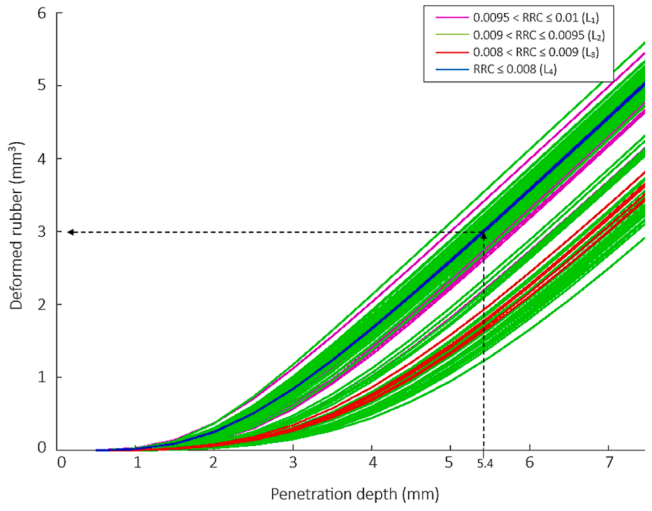

Fig. 4.10. Volume of deformed rubber for a range of penetration depths based on rolling resistance coefficient.

techniques improved model performance and predictive accuracy, it is important to note that the dataset used was relatively small and the RRC range was narrow (0.008–0.01). Therefore, caution should be exercised in generalizing these findings to broader datasets or wider RRC ranges, and further studies with larger and more diverse data are recommended.

iii. *Investigation of machine learning-based models:* Given the limitations of regression-based models, ML techniques showed improved prediction accuracy, as indicated by relatively high R^2, low MSE and low MAE values. The ML-MLR model showed slightly improved prediction accuracy compared to commonly used models under excluding the varied sampling technique, indicating its inability to capture the nonlinear relationships between features and *RRC*. In contrast, the RF model demonstrated better performance, effectively capturing complex nonlinear relationships and significantly reducing prediction error.

iv. *Investigation of automatic tire penetration calculation framework using LCMS data:* Cluster patterns in the LCMS dataset demonstrated that newer pavements exhibited lower *RRC* values compared to older pavements, reinforcing the hypothesis that surface deterioration increases rolling resistance. The study shows that as the tire penetration depth increases, the volume of deformed rubber also increases, validating the reliability of the methodology used for penetration depth analysis through LCMS data. However, no clear correlation was found between the volume of deformed rubber and penetration depth within the examined *RRC* dataset.

Overall, the study shows that traditional statistical models have limited predictive capability for rolling resistance due to their inability to account for nonlinear relationships. The implementation of varied data sampling techniques improves predictive accuracy but remains insufficient. Advanced ML models, particularly RF, significantly enhance prediction performance and provide a reliable framework for future studies on rolling resistance estimation. To further improve prediction accuracy, a more extensive experimental dataset related to physical information of tire-pavement interaction should be considered for further refinement, along with an enhanced ML toolkit. The findings of this study underscore the importance of ML techniques in overcoming

the challenges associated with conventional rolling resistance prediction models, paving the way for more accurate and efficient assessments in pavement engineering.

6. Future research directions

The study provides the pathway for several promising future directions of rolling resistance prediction in terms of both tire and pavement characteristics. Further investigations by integrating additional data sources, such as stiffness modulus of the asphalt pavement layer, age of the pavement, real-time traffic data, weather data, tire related data, and data of vehicle operating condition could provide a more comprehensive understanding of rolling resistance dynamics in varied conditions. In addition, incorporating tire pavement interaction factors with ML algorithms could offer better prediction accuracy of rolling resistance while helping to development of robust and automated predictive models.

CRediT authorship contribution statement

W.A.A.S. Premarathna: Writing – review & editing, Writing – original draft, Visualization, Validation, Software, Methodology, Investigation, Formal analysis, Data curation. **Kumar Anupam:** Writing – review & editing, Writing – original draft, Supervision, Resources, Project administration, Methodology, Investigation. **M. Moenielal:** Writing – review & editing, Supervision, Software, Resources, Project administration, Investigation, Formal analysis, Data curation. **Thijs Wensveen:** Visualization, Software, Formal analysis, Data curation. **Cor Kasbergen:** Writing – review & editing, Supervision, Resources, Project administration, Methodology, Investigation, Funding acquisition. **Sandra M.J.G. Erkens:** Supervision, Resources, Project administration, Investigation, Funding acquisition.

Declaration of competing interest

The authors declare the following financial interests/personal relationships which may be considered as potential competing interests:

Kumar Anupam reports financial support was provided by Rijkswaterstaat (RWS). If there are other authors, they declare that they have no known competing financial interests or personal relationships that could have appeared to influence the work reported in this paper.

Acknowledgment

The authors gratefully acknowledge the support received from the Knowledge-based Pavement Engineering (KPE) research program. KPE is a collaborative initiative involving Rijkswaterstaat, TNO, and TU Delft, aimed at advancing scientific and applied knowledge in the field of asphalt pavements. The authors would also like to acknowledge the significant contributions of Bram Vreugdenhil and Harco Kersten of Rijkswaterstaat, whose expertise and support were essential to this work. Furthermore, this research contributes to Rijkswaterstaat's ambitious objectives of achieving complete climate neutrality and embracing circular principles by 2030.

Data availability

The authors do not have permission to share data.

References

[1] I. Arora et al., "Technologies for hydrogen production from fossil fuels and hydrocarbons," 2023.
[2] P. Friedlingstein, M. O'Sullivan, M.W. Jones, R.M. Andrew, D.C. Bakker, J. Hauck, B. Zheng, Global carbon budget 2023, Earth. Syst. Sci. Data 15 (12) (2023) 5301–5369, https://doi.org/10.5194/essd-15-5301-2023.
[3] NOAA National Centers for Environmental Information, Monthly global climate report for annual, published online Jan. 2024, retrieved Apr. 12, https://www.ncei.noaa.gov/access/monitoring/monthly-report/global/202300, 2024.
[4] UNEP United Nations Environment Programme, *Emissions Gap Report 2023: broken record temperatures hit new highs, yet world fails to cut emissions (again)*, Nairobi, 2023. doi: 10.59117/20.500.11822/43922.
[5] W.F. Lamb, T. Wiedmann, J. Pongratz, R. Andrew, M. Crippa, J.G. Olivier, J. Minx, A review of trends and drivers of greenhouse gas emissions by sector from 1990 to 2018, Environ. Res. Lett. 16 (7) (2021) 073005.
[6] E. Lindstad, T.Ø. Ask, P. Cariou, G.S. Eskeland, A. Rialland, Wise use of renewable energy in transport, Transp. Res. D: Transp. Environ. 119 (2023) 103713.
[7] J.S. Kikstra, Z.R. Nicholls, C.J. Smith, J. Lewis, R.D. Lamboll, E. Byers, K. Riahi, The IPCC Sixth Assessment Report WGIII climate assessment of mitigation pathways: from emissions to global temperatures, Geosci. Model. Dev. 15 (24) (2022) 9075–9109.
[8] C.A. Romero, P. Correa, E.A. Ariza Echeverri, D. Vergara, Strategies for reducing automobile fuel consumption, Appl. Sci. 14 (2) (2024) 910.
[9] R. Jiang, P. Wu, C. Wu, Driving factors behind energy-related carbon emissions in the US road transport sector: a decomposition analysis, Int. J. Environ. Res. Public Health 19 (4) (2022) 2321.
[10] Z. Sun, W.A.A.S. Premarathna, K. Anupam, C. Kasbergen, S.M. Erkens, A state-of-the-art review on rolling resistance of asphalt pavements and its environmental impact, Constr. Build. Mater. 411 (2024) 133589, https://doi.org/10.1016/j.conbuildmat.2023.133589.
[11] J. Chun, J. McKeown, S. Kang, Impact of vehicle electrification on road roughness induced greenhouse gas (GHG) emissions, Sustain. Energy Technol. Assess 64 (2024) 103701, https://doi.org/10.1016/j.seta.2024.103701.
[12] European Parliament, On the monitoring and reporting of CO2 emissions from and fuel consumption of new heavy-duty vehicles, Jun. 18, https://eur-lex.europa.eu/legal-content/EN/TXT/?uri=CELEX%3A32018R0956, 2018.
[13] W. Levesque, A. Bégin-Drolet, J. Lépine, Effects of pavement characteristics on rolling resistance of heavy vehicles: a literature review, Transp. Res. Rec. 2677 (6) (2023) 296–309, https://doi.org/10.1177/03611981221145125.
[14] L. Trupia, T. Parry, L.C. Neves, D.L. Presti, Rolling resistance contribution to a road pavement life cycle carbon footprint analysis, Int. J. Life Cycle Assess. 22 (2017) 972–985, https://doi.org/10.1007/s11367-016-1203-9.
[15] S. Chen, et al., A state-of-the-art review of asphalt pavement surface texture and its measurement techniques, J. Road Eng. 2 (2) (2022) 156–180, https://doi.org/10.1016/j.jreng.2022.05.003.
[16] U. Hammarström, J. Eriksson, R. Karlsson, M.R. Yahya, Rolling Resistance model, Fuel Consumption Model and the Traffic Energy Saving Potential from Changed Road Surface Conditions, Statens väg-och transportforskningsinstitut, 2012.
[17] J. Hooghwerff, E.W. van Gils, and H.F. Reinink, "Influence of road surface type on rolling resistance," 2013.
[18] S. Boere, I.L. Arteaga, A. Kuijpers, H. Nijmeijer, Tyre/road interaction model for the prediction of road texture influence on rolling resistance, Int. J. Veh. Des. 65 (2–3) (2014) 202–221, https://doi.org/10.1504/IJVD.2014.060815.
[19] I. Zaabar, K. Chatti, Estimating vehicle operating costs caused by pavement surface conditions, Transp. Res. Rec. 2455 (1) (2014) 63–76, https://doi.org/10.3141/2455-08.
[20] H.R. Kerali, J.B. Odoki, D.C. Wightman, E.E. Stannard, Structure of the new highway development and management tools HDM-4, in: Fourth International Conference on Managing Pavements 2, 1998, pp. 961–973. May.
[21] U. Sandberg, A. Bergiers, J.A. Ejsmont, L. Goubert, R. Karlsson, and M. Zöller, "Road surface influence on tyre/road rolling resistance," ORCID iD: 0009-0003-2678-6961, 2011.
[22] J.R. Willis, M.M. Robbins, and M. Thompson, "Effects of pavement properties on vehicular rolling resistance: a literature review," Report 14-07, 2015.
[23] M. Fakhri, S.M. Karimi, J. Barzegaran, Predicting international roughness index based on surface distresses in various climate and traffic conditions using laser crack measurement system, Transp. Res. Rec. 2675 (11) (2021) 397–412, https://doi.org/10.1177/03611981211017906.
[24] J. Laurent, D. Lefebvre, E. Samson, Y. Savard, M. Grondin, Implementation and validation of a new 3D automated pavement cracking measurement equipment, in: Proc., 11th International Conference on Asphalt Pavements International Society for Asphalt Pavements, Nagoya, Japan, 2010.
[25] G. Descornet, Road-surface influence on tire rolling resistance. Surface Characteristics of roadways: International Research and Technologies, ASTM International, 1990.
[26] U. Sandberg, U. Hammarström, M. Haider, M. Conter, L. Goubert, A. Bergiers, … and J.T. Harvey, "Rolling resistance: basic information and state-of-the-art on measurement methods," Final version, 2011.
[27] R. Spielhofer, ROSANNE-rolling resistance, skid resistance and noise emission measurement standards for road surfaces, Eur. Road Profile Users Group Forum (2013).
[28] J.A. Ejsmont, G. Ronowski, B. Świeczko-Żurek, S. Sommer, Road texture influence on tyre rolling resistance, Road Mater. Pavement Des. 18 (1) (2017) 181–198, https://doi.org/10.1080/14680629.2016.1160835.
[29] E. Riahi, C. Ropert, M.T. Do, Developing a laboratory test method for rolling resistance characterisation of road surface texture, Surf. Topogr. Metrol. Prop. 8 (2) (2020) 024006, https://doi.org/10.1088/2051-672X/ab8aa6.
[30] M. Kane, E. Riahi, M.T. Do, Tire/road rolling resistance modeling: discussing the surface macrotexture effect, Coatings 11 (5) (2021) 538, https://doi.org/10.3390/coatings11050538.

[31] J. Ejsmont, S. Sommer, Selected aspects of pavement texture influence on tire rolling resistance, Coatings 11 (7) (2021) 776, https://doi.org/10.3390/coatings11070776.
[32] L.G. Andersen, Rolling Resistance Modelling: From Functional Data Analysis to Asset Management System, Roskilde Univ., Denmark, 2015. Ph.D. dissertation.
[33] A. Koné, A. Es-Sabar, M.T. Do, Application of machine learning models to the analysis of skid resistance data, Lubricants. 11 (8) (2023) 328.
[34] H. Li, R. Nyirandayisabye, Q. Dong, R. Niyirora, T. Hakuzweyezu, I.A. Zardari, F. Nkinahamira, Crack damage prediction of asphalt pavement based on tire noise: a comparison of machine learning algorithms, Constr. Build. Mater. 414 (2024) 134867, https://doi.org/10.1016/j.conbuildmat.2024.134867.
[35] G. Biau, Analysis of a random forests model, J. Mach. Learn. Res. 13 (1) (2012) 1063–1095.
[36] R. Nyirandayisabye, H. Li, Q. Dong, T. Hakuzweyezu, F. Nkinahamira, Automatic pavement damage predictions using various machine learning algorithms: evaluation and comparison, Results. Eng. 16 (2022) 100657.
[37] C.N. Van, D.N. Tran, T.T. Long, N.G.M. Thao, D.T. Tran, Hybrid feature selection for real-time road surface classification on low-end hardware: a machine learning approach, Results. Eng. (2025) 105693.
[38] S. Cano-Ortiz, P. Pascual-Munoz, D. Castro-Fresno, Machine learning algorithms for monitoring pavement performance, Autom. Constr. 139 (2022) 104309, https://doi.org/10.1016/j.autcon.2022.104309.
[39] I. Uva, J. Santos, V. Cerezo, S. Miller, RolRoad–LCA: a web-based application for estimating the excess fuel consumption and environmental impacts due to the rolling resistance of passenger cars, in: International Symposium on Pavement, Roadway, and Bridge Life Cycle Assessment, Cham, Springer Nature Switzerland, 2024, pp. 69–77, https://doi.org/10.1007/978-3-031-61585-6_8. May.
[40] Z. Wang, P. Krishnakumari, K. Anupam, H. van Lint, S. Erkens, A causal discovery approach to study key mixed traffic-related factors and age of highway affecting raveling, Comput.-Aided Civ. Infrastruct. Eng. (2024), https://doi.org/10.1111/mice.13222.
[41] D. Wang, A. Ueckermann, A. Schacht, M. Oeser, B. Steinauer, Relationship between the tire penetration depth and the road surface texture: a theoretical model and its practical application, Des. Anal. Asph. Mater. Charact. Road Airf. Pavements (2014) 32–40.
[42] P. Farhadi, A. Golmohammadi, A.S. Malvajerdi, G. Shahgholi, Prediction of the tractor tire contact area, contact volume and rolling resistance using regression model and artificial neural network, Agric. Eng. Int. CIGR J. 21 (3) (2019) 26–38.
[43] D.F. De Graaff, J. Hooghwerff, E.W. van Gils, and H.F. Reinink, "Influence of road surface type on rolling resistance: rolling resistance measurement programme 2012," M+P report DVS.12.04.2 rev.5, Oct. 22, 2012.
[44] X. Chen, H. Zheng, H. Wang, T. Yan, Can machine learning algorithms perform better than multiple linear regression in predicting nitrogen excretion from lactating dairy cows, Sci. Rep. 12 (1) (2022) 12478.
[45] B.N. Persson, Theory of rubber friction and contact mechanics, J. Chem. Phys. 115 (8) (2001) 3840–3861, https://doi.org/10.1063/1.1388626.
[46] B.N. Persson, O. Albohr, U. Tartaglino, A.I. Volokitin, E. Tosatti, On the nature of surface roughness with application to contact mechanics, sealing, rubber friction and adhesion, J. Phys. Condens. Matter. 17 (1) (2004) R1, https://doi.org/10.1088/0953-8984/17/1/R01.
[47] A. Ueckermann, D. Wang, M. Oeser, B. Steinauer, Calculation of skid resistance from texture measurements, J. Traffic Transp. Eng. 2 (1) (2015) 3–16, https://doi.org/10.1016/j.jtte.2015.01.001.
[48] A. Alhasan, O. Smadi, G. Bou-Saab, N. Hernandez, E. Cochran, Pavement friction modeling using texture measurements and pendulum skid tester, Transp. Res. Rec. 2672 (40) (2018) 440–451, https://doi.org/10.1177/0361198118774165.
[49] M.M. Kanafi, A.J. Tuononen, Top topography surface roughness power spectrum for pavement friction evaluation, Tribol. Int. 107 (2017) 240–249, https://doi.org/10.1016/j.triboint.2016.11.038.
[50] W. Guo, L. Chu, L. Yang, T.F. Fwa, Determination of tire rubber-pavement directional coefficient of friction based on contact mechanism considerations, Tribol. Int. 179 (2023) 108178, https://doi.org/10.1016/j.triboint.2022.108178.
[51] B. Lorenz, Contact Mechanics and Friction of Elastic Solids On Hard and Rough Substrates, 37, Forschungszentrum Jülich, 2012.
[52] B.N. Persson, On the theory of rubber friction, Surf. Sci. 401 (3) (1998) 445–454, https://doi.org/10.1016/S0039-6028(98)00051-X.
[53] S. Ding, K.C. Wang, E. Yang, Y. Zhan, Influence of effective texture depth on pavement friction based on 3D texture area, Constr. Build. Mater. 287 (2021) 123002, https://doi.org/10.1016/j.conbuildmat.2021.123002.
[54] D. Yun, C. Tang, U. Sandberg, M. Ran, X. Zhou, J. Gao, L. Hu, A new approach for determining rubber enveloping on pavement and its implications for friction estimation, Coatings 14 (3) (2024) 301.
[55] D. Wang, A. Ueckermann, A. Schacht, M. Oeser, B. Steinauer, B.N.J. Persson, Tire–road contact stiffness, Tribol. Lett. 56 (2014) 397–402, https://doi.org/10.1007/s11249-014-0417-x.
[56] L. Goubert, U. Sandberg, Enveloping texture profiles for better modelling of the rolling resistance and acoustic qualities of road pavements, in: Symposium on Pavement Surface Characteristics (SURF), 8th, Brisbane, Queensland, Australia, 2018. May.
[57] L. Yang, L. Chu, B. Zhou, W. Guo, T.F. Fwa, Characterizing directional traffic-induced wear of road pavements, Wear. 488 (2022) 204129, https://doi.org/10.1016/j.wear.2021.204129.
[58] L. Chu, B. Zhou, T.F. Fwa, Directional characteristics of traffic polishing effect on pavement skid resistance, Int. J. Pavement Eng. 23 (9) (2022) 2937–2953, https://doi.org/10.1080/10298436.2021.1874378.
[59] J.C. Huang, K.M. Ko, M.H. Shu, B.M. Hsu, Application and comparison of several machine learning algorithms and their integration models in regression problems, Neural Comput. Appl. 32 (10) (2020) 5461–5469.
[60] X. Xie, T. Wu, M. Zhu, G. Jiang, Y. Xu, X. Wang, L. Pu, Comparison of random forest and multiple linear regression models for estimation of soil extracellular enzyme activities in agricultural reclaimed coastal saline land, Ecol. Indic. 120 (2021) 106925.
[61] D. Kinaneva, G. Hristov, P. Kyuchukov, G. Georgiev, P. Zahariev, R. Daskalov, Machine learning algorithms for regression analysis and predictions of numerical data, in: 2021 3rd International Congress on Human-Computer Interaction, Optimization and Robotic Applications (HORA), IEEE, 2021, pp. 1–6. June.
[62] Y. Hu, Z. Sun, Y. Han, W. Li, L. Pei, Evaluate pavement skid resistance performance based on Bayesian-LightGBM using 3D surface macrotexture data, Mater 15 (15) (2022) 5275, https://doi.org/10.3390/ma15155275.
[63] L.S. Iyer, AI enabled applications towards intelligent transportation, Transp. Eng. 5 (2021) 100083, https://doi.org/10.1016/j.treng.2021.100083.
[64] T.H. Le, H.L. Nguyen, B.T. Pham, M.H. Nguyen, C.T. Pham, N.L. Nguyen, H.B. Ly, Artificial intelligence-based model for the prediction of dynamic modulus of stone mastic asphalt, Appl. Sci. 10 (15) (2020) 5242, https://doi.org/10.3390/app10155242.
[65] T. Long, Z. Zhou, G. Hancke, Y. Bai, Q. Gao, A review of artificial intelligence technologies in mineral identification: classification and visualization, J. Sens. Actuator Netw. 11 (3) (2022) 50, https://doi.org/10.3390/jsan11030050.
[66] R. Bayat, S. Talatahari, A.H. Gandomi, M. Habibi, B. Aminnejad, Artificial Neural networks for flexible pavement, Information 14 (2) (2023) 62, https://doi.org/10.3390/info14020062.
[67] P. Marcelino, M. de Lurdes Antunes, E. Fortunato, M.C. Gomes, Machine learning approach for pavement performance prediction, Int. J. Pavement Eng. 22 (3) (2021) 341–354, https://doi.org/10.1080/10298436.2019.1609673.
[68] Y. Zhan, C. Liu, Q. Deng, Q. Feng, Y. Qiu, A. Zhang, X. He, Integrated FFT and XGBoost framework to predict pavement skid resistance using automatic 3D texture measurement, Measurement 188 (2022) 110638.
[69] G. Yang, W. Yu, Q.J. Li, K. Wang, Y. Peng, A. Zhang, Random forest–based pavement surface friction prediction using high-resolution 3D image data, J. Test. Eval. 49 (2) (2021) 1141–1152.
[70] E. Golov, S. Evtyukov, M. Protsuto, S. Evtyukov, E. Sorokina, Influence of the road surface roughness (according to the International Roughness Index) on road safety, Transp. Res. Procedia. 63 (2022) 999–1006.
[71] H. Gong, Y. Sun, X. Shu, B. Huang, Use of random forests regression for predicting IRI of asphalt pavements, Constr. Build. Mater. 189 (2018) 890–897.
[72] M.Z. Bashar, C. Torres-Machi, Performance of machine learning algorithms in predicting the pavement international roughness index, Transp. Res. Rec. 2675 (5) (2021) 226–237.
[73] W. Guo, J. Zhang, D. Cao, H. Yao, Cost-effective assessment of in-service asphalt pavement condition based on random forests and regression analysis, Constr. Build. Mater. 330 (2022) 127219.
[74] N. Sholevar, A. Golroo, S.R. Esfahani, Machine learning techniques for pavement condition evaluation, Autom. Constr. 136 (2022) 104190.
[75] W.V. Aalst, G. Derksen, P.P. Schackmann, P. Paffen, F. Bouman, W.V. Ooijen, Automated ravelling inspection and maintenance planning on porous asphalt in the Netherlands, in: International Symposium Non-Destructive Testing in Civil Engineering (NDTCE), Berlin, Germany, 2015. Sep.
[76] B. Świeczko-Żurek, G. Ronowski, J. Ejsmont, Tyre rolling resistance and its influence on fuel consumption, Combust Engines 168 (2017) 62–67, https://doi.org/10.19206/CE-2017-110.
[77] Rijkswaterstaat, "Wegenoverzicht - informatie en data," *Rijkswaterstaat*, [Online]. Available: https://www.rijkswaterstaat.nl/wegen/wegenoverzicht.
[78] J. Laurent, J. Hébert, M. Talbot, Using full lane 3D road texture data for the automated detection of sealed cracks, bleeding and ravelling, in: Proceedings of the World Conference on Pavement and Asset Management, Milan, Italy, 2017, pp. 12–16. June.
[79] ISO, Characterization of Pavement Texture By Use of Surface Profiles — Part 1: Determination of Mean Profile Depth, 2nd ed., ISO Standard 13473-1, 2019. Feb.
[80] GREGORY Technology GmbH, Correvit® L-350 Aqua Non-contact optical sensor, Accessed February 5, https://www.flowtronic.de/products/distance-sensors/l-350-aqua.html, 2025.
[81] LMI Technologies, LMI laser 2207-64/180-G, Accessed February 5, https://lmi3d.com, 2025.
[82] P.R. Donavan, "Use of the ASTM standard reference test tire as a benchmark for on-board tire/pavement noise measurement," *SAE Technical Paper*, 2009, no. 2009-01-2108.
[83] R.A. Armstrong, F. Eperjesi, B. Gilmartin, The application of analysis of variance (ANOVA) to different experimental designs in optometry, Ophthalmic. Physiol. Opt. 22 (3) (2002) 248–256.
[84] B. Baumann, C.W. Merkle, R.A. Leitgeb, M. Augustin, A. Wartak, M. Pircher, C. K. Hitzenberger, Signal averaging improves signal-to-noise in OCT images: but which approach works best, and when? Biomed. Opt. Express. 10 (11) (2019) 5755–5775.
[85] P. Ciotirnae, C. Dumitrescu, I.C. Chiva, A. Semenescu, E.C. Popovici, D. Dranga, Method for noise reduction by averaging the filtering results on circular displacements using wavelet transform and local binary pattern, Electron 13 (20) (2024) 4119.
[86] L. Berre, G. Desroziers, Filtering of background error variances and correlations by local spatial averaging: a review, Mon. Weather. Rev. 138 (10) (2010) 3693–3720.
[87] F. Pedregosa, G. Varoquaux, A. Gramfort, V. Michel, B. Thirion, O. Grisel, M. Blondel, A. Müller, J. Nothman, G. Louppe, P. Prettenhofer, R. Weiss,

V. Dubourg, J. VanderPlas, A. Passos, D. Cournapeau, M. Brucher, M. Perrot, É. Duchesnay, Comparing randomized search and grid search for hyperparameter estimation, Scikit-Learn (2025) [Online]. Available, https://scikit-learn.org/stable/auto_examples/model_selection/plot_randomized_search.html [Accessed: 02-Jan-2025].

[88] S. Elf and C. Öqvist, "Comparison of supervised machine learning models for predicting TV-ratings," 2020.

[89] F.G. Praticò, R. Vaiana, A study on the relationship between mean texture depth and mean profile depth of asphalt pavements, Constr. Build. Mater. 101 (2015) 72–79.

[90] K. Kamiya, R. Kato, D. Matsumoto, S. Motomatsu, T. Tanaka, K. Yamaguchi, Long lasting durable mix as alternative of porous asphalt, in: Proc. 24th World Road Congress, World Road Association (PIARC), 2011.

[91] B. Chen, P. Ding, G. Wei, C. Xiong, F. Wang, J. Yu, Y. Zou, A study on the contact characteristics of tires–roads based on pressure-sensitive film technology, Mater 16 (18) (2023) 6323.